

University of Richmond

UR Scholarship Repository

Honors Theses

Student Research

2016

Structure-function relationships affecting the sensing mechanism of monolayer-protected cluster doped xerogel amperometric glucose biosensors

Luke T. DiPasquale
University of Richmond

Follow this and additional works at: <https://scholarship.richmond.edu/honors-theses>

 Part of the [Chemistry Commons](#)

Recommended Citation

DiPasquale, Luke T., "Structure-function relationships affecting the sensing mechanism of monolayer-protected cluster doped xerogel amperometric glucose biosensors" (2016). *Honors Theses*. 944.
<https://scholarship.richmond.edu/honors-theses/944>

This Thesis is brought to you for free and open access by the Student Research at UR Scholarship Repository. It has been accepted for inclusion in Honors Theses by an authorized administrator of UR Scholarship Repository. For more information, please contact scholarshiprepository@richmond.edu.

Structure-Function Relationships Affecting the Sensing Mechanism of Monolayer-Protected Cluster Doped Xerogel Amperometric Glucose Biosensors

by

Luke T. DiPasquale

Honors Thesis

Submitted to

*Department of Chemistry, Gottwald Center for the Sciences
University of Richmond
Richmond, VA*

April 25, 2016

Advisor: Dr. Michael Leopold

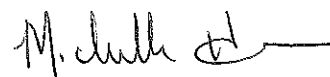
APPROVED BY:

ADVISOR



**Dr. Michael Leopold
Department of Chemistry
University of Richmond**

SECOND READER



**Dr. Michelle Hamm
Department of Chemistry
University of Richmond**

DEDICATION

I would like to dedicate the following to a few very influential individuals. First and foremost, this work is dedicated to my parents, Tom and Karen DiPasquale, for their unconditional love and support throughout my entire life, especially during my time in college. Without their hard work and dedication to their four children, I would not have had the opportunity to attend such a prestigious university and conduct the research that I have for the past four years. They are my inspiration in every sense of the word, and are the reason I have a drive and passion for making the world a better place. This work is also dedicated to my brothers Zachary and Patrick DiPasquale and my sister Natalie DiPasquale for teaching me the value of family and inspiring me to be the best student and friend I can be. Lastly, I would like to dedicate this work to my first chemistry professor at the University of Richmond, my senior seminar and research advisor, my colleague, and my dear friend, Dr. Michael Leopold, for being an outstanding professor and mentor, for challenging me as a first-year student to find a love for chemistry, and for going above and beyond as a research advisor and a mentor during my four years at the University of Richmond.

TABLE OF CONTENTS

Dedication	ii
Table of Contents	iii
Acknowledgements	iv
Abstract	v
1. Introduction	1
2. Experimental	5
2.1 – Nanoparticle Synthesis and Functionalization	
2.2 – Preparation of MPC – Doped Xerogel Film Sensors	
2.3 – Biosensor Performance and Electrochemical Film Characterization	
2.4 – Electronic Conductivity Measurements	
3. Results and Discussion	8
3.1 – Chain Length of the MPC Peripheral Ligands	
3.2 – Functionalization of the MPC Peripheral Ligands	
3.3 – MPC Core Size	
3.4 – Composite Xerogel-MPC Films	
4. Conclusion	24
Appendix	26
References	33

ACKNOWLEDGEMENTS

This research was supported by funding from the National Science Foundation (CHE-1401593), Virginia's Commonwealth Health Research Board, and Henry Dreyfus Teacher-Scholar Award Program, as well as student fellowships from the University of Richmond's Undergraduate Research Committee and Chemistry Department Puryear-Topham-Gupton-Pierce Fund (LTD, NGP, AM, and TAB). I would like to thank Nicholas G. Poulos, Jackson R. Hall, Aastha Minocha, and Tram Anh Bui for their vital contributions to this work, and a special acknowledgment to Michael C. Leopold for his oversight of all projects. Our group would also like to thank Dr. Jonathan Dattelbaum, University of Richmond, for his helpful discussions. We also gratefully acknowledge the following people for making research possible at the University of Richmond: Drs. T. Leopold, R. Kanters, D. Kellogg, R. Miller, and W. Case, as well as Christie Davis, Russ Collins, Phil Joseph, Mandy Mallory, and Lamont Cheatham.

ABSTRACT

The research conducted in the Leopold Bioanalytical and Nanomaterials Analytical Chemistry Lab prior to the summer of 2013 focused on the synthesis of a functional biosensor equipped with a nanoparticle network embedded in a xerogel film for the detection of glucose. Xerogel-based films featuring embedded glucose oxidase enzyme and doped with alkanethiolate-protected gold NPs, known as monolayer protected clusters (MPCs), exhibit significantly enhanced performance compared to analogous systems without NPs including higher sensitivity, faster response time, and extended linear/dynamic ranges.

The following presented research is a systematic study of the structure-function relationships critical to understanding the sensing mechanism of the 1st generation glucose biosensor with an embedded nanoparticle (NP) network. The proposed mechanism involves diffusion of the glucose to glucose oxidase enzyme within the xerogel, enzymatic reaction production of H₂O₂ with subsequent diffusion to the embedded network of MPCs where it is oxidized, an event immediately reported via fast electron transfer (ET) through the MPC system to the working electrode. To confirm our theory, various aspects of the film construct and strategy are systematically probed using amperometry, voltammetry, and solid-state electronic conductivity measurements, including the effects of MPC peripheral chain length, MPC functionalization via place-exchange reaction, MPC core size, and the MPC density or concentration within the xerogel composite films.

The results of these experiments support the proposed mechanism and identify interparticle spacing and the electronic communication through the MPC network as the most significant factors in the sensing scheme with the diffusional aspects of the mechanism that may be affected by film/MPC hydrophobicity and functionality (i.e., glucose and H₂O₂ diffusion) shown to be less substantial contributors to the overall enhanced performance. The importance of understanding the mechanism behind the enhanced performance of MPC doped xerogel biosensors is for its application for future biosensor design toward clinically relevant targets.

1. INTRODUCTION

Biosensor research represents an important and expanding sector of materials and interfacial chemistry due to their many and varied applications across disciplines. Electrochemical sensor development continues to draw a significant level of interest as it remains relatively simple and affordable while still maintaining the potential for adaptability to different analytes relevant for both clinical and industrial applications.[1-3] In particular, 1st generation amperometric biosensors, which utilize immobilized enzymes to catalyze an analyte to hydrogen peroxide (H₂O₂) that is then subsequently oxidized at the working electrode to produce a current response representative of analyte concentration, continue to receive attention due to their ability to provide increased sensitivity, analyte selectivity and quick response times with the potential of miniaturization leading to *in vitro* remote sensing as well as *in vivo* applications.[1]

In a 1st generation biosensing model, the enzyme must be immobilized without compromising structural integrity of the sensor or the inhibiting enzyme function. Sol-gels represent an appealing method of immobilization because they easily and without harsh conditions form a rigid silicate network that is both chemically inert and resistant to significant swelling in the presence of water but able to maintain enzyme activity.[4] When cast from solvent and allowed to age under controlled humidity and temperature, the sol-gels formed are known as xerogels.[5, 6] The expansive catalogue of silanes allows for a multitude of xerogels to be constructed for specific chemistry. For example, 3-mercaptopropyltrimethoxy silane (3-MPTMS) introduces thiol functionality into the gels where it has been used to bind certain metallic nanomaterials (NMs).[7, 8] Among their other properties, the ability of NMs to aid in electron transfer (ET) processes has made NP-assisted biosensor designs increasingly prevalent in the field. The multitude of different nanomaterials allows for possible specialization of a biosensor depending on their specific size, shape and composition.[3]

Literature reports suggest that the use of certain NMs, specifically metallic nanoparticles (NPs), allow for greater microenvironment control through the creation of a NP network that enhances the ET from reaction site to the electrode.[9, 10] A major focus of that body of work is on the use of colloidal gold NPs as a component of electrochemical biosensors. Most of these reports focus on proof-of-concept rather than exploring the role of NP structure in the sensor performance and functionality.[11-16] Few, if any, of these reports adequately focus on mechanistic understanding the NPs within their sensing schemes.

In 2013, a 1st generation amperometric glucose biosensor model system featuring a MPTMS xerogel embedded with glucose oxidase (GOx) and doped with gold NPs known as monolayer protected clusters (MPC) was demonstrated.[8] The composite MPC-doped xerogel film was deposited on a platinum electrode and coated with a semi-permeable polyurethane (PU) layer to assist in interferent discrimination (**Scheme I**). The study explored majorly the effects of incorporating a nanoparticle network into the sensor scheme, and was a comparative performance analysis between systems with an MPC network and systems without MPCs on the basis of sensitivity, linear dynamic range, and response time with an additional focus on stability and selectivity of the separate sensor systems. This work focused on permeability of both the polyurethane protective layer, as well as the sol-gel matrix. The study tested varied polyurethane ratios of HPU:TPU (100mg HPU : 0mg TPU, 75mg HPU : 25mg TPU, 50mg HPU : 50mg TPU, 25mg HPU : 75mg TPU, and 0mg HPU : 100mg TPU) for their response to the interfering analytes of ascorbic acid, acetaminophen, sodium nitrite, oxalic acid and uric acid. The study also focused on the differences between bare, sol-gel modified, polyurethane modified, and sol-gel/polyurethane modified systems for their interferent responses as well as their response to the standard glucose injection. The results of this study identify an MPC-doped xerogel film with a

50:50 HPU:TPU ratio polyurethane protective layer to be the ideal system showing an order of magnitude increase in sensitivity, doubled linear range, and a 4-fold decrease in response times compared to similar sensors without MPCs (**Figure 1**), as well as better overall selectivity and stability as compared to values in the literature. While the enhanced performance and characterization of this model system was well-documented and compared with other literature reports of similar sensors with and without NMs, a mechanistic understanding of the structure-function relationships involving the embedded MPCs was not a major focus of the study.

More recent work[17] investigated the functionality of the layered approach, including the specific role of the silane precursor material and polyurethane, but did not connect the findings to the MPC-doped xerogels. This study tested layered systems equipped with varied silane ratios for their response to glucose, providing strong evidence of an optimal silane recipe dependent upon the analyte targeted for detection.

In this paper, we follow up these important findings with the systematic interrogation of MPC characteristics within the doped xerogels including core size, ligand chain length, and ligand functionality, with an aim of establishing the critical structure-function relationships in these composite materials that are responsible for the observed sensing enhancement[8] and that may help shape a proposed sensing mechanism.

Clinical application and incorporation is a major goal of the research group when designing sensors. The focus of the following research was to propose and support a theoretical mechanism for the electron transfer through the successful MPC-doped system, in order to better understand the role that the MPCs play within the film. Identifying and understanding the mechanism of electron transfer within this sensing scheme allows for the subsequent application to other sensors. While the lab has succeeded in generating a sensor for detecting levels of glucose at varied

concentrations, current and future projects are focused on the development of sensors for detecting levels of lactate, uric acid, and galactose.

Sepsis and septic shock are common conditions in patients with severe degrees of infection. In the United States alone, sepsis affects more than one million patients each year, and kills between 28-50% of those patients, according to the National Institute of Health [41]. Characterized by high levels of lactate within the bloodstream, it is a treatable condition if identified. However, the current method of lactate detection is via blood diagnostic tests, which can delay detection and thereby increase a patient's chance of developing sepsis. The ideal method of identification would be an instantaneous, real-time monitor of lactate levels in the bloodstream.

Pregnancy-Induced Hypertension (PIH), also known as preeclampsia, is a common hypertensive disorder that affects nearly 200,000 women each year, approximately four percent of all pregnancies. The National Institute of Health reports that PIH and other hypertensive disorders are the cause of death in approximately 76,000 women and 500,000 infants each year [42]. It is caused by dangerously high levels of uric acid produced around the 20th week of the pregnancy. Though not always fatal, PIH is a serious condition that can lead to complications for both the baby and the mother if not treated properly, or detected at an early enough stage. PIH is a very treatable condition, but, like lactate, its detection in current medical settings requires diagnostic tests on blood samples, a tedious process that can take hours to return to the physician. The development of a uric acid biosensor that can instantaneously detect hyperurecemia would help physicians to identify the need for immediate interventions to counter the condition, and would thus reduce the number of affected women and children each year.

Hypergalactosemia is another condition in infants caused by a genetic disorder that results in the inability to produce the enzyme that breaks down galactose, a by-product of the breakdown

of lactose. In infants, this is a dangerous condition that can lead to liver failure, sepsis, and even neonatal death if not managed properly. If not identified at an early stage, the condition can also lead to delays in development, speech problems, and motor function complications [43]. Again, the detection of this condition is an identification of high levels of galactose in the infant bloodstream, but can currently only be detected by blood diagnostics tests. The development of a sensor for the detection of this analyte would be very effective in reducing the number of infants affected by this condition.

The relevance of understanding the proposed MPC-doped sensor mechanism hereafter becomes apparent. Understanding the mechanism behind the electron transfer can allow us to modify the system to meet the needs of the variations between the different analytes, a critical task for the development of future sensors.

2. EXPERIMENTAL

2.1 - Nanoparticle Synthesis and Functionalization

Alkanethiolate-protected MPC's were synthesized using variations of the established Brust reaction.[18, 19] The final product, a black solid dust, was characterized using NMR, UV-Vis, and TEM imaging with Image J histogram analysis to confirm the *average* core composition and diameter of Au₂₂₅ and 2.03 ± 0.95 nm. Various thiol-to-gold ratios of 4:1, 3:1, 2:1, 1:1, and 1:12 and other reaction conditions were used modify the Brust synthesis to produce MPC's with *average* cores of Au₇₉, Au₁₄₄, Au₂₂₅, Au₃₁₄, and Au₄₇₉₄ respectively.[20]

Functionalized MPC's were generated via well-known place-exchange techniques.[21] NMR spectroscopy of iodine treated functionalized MPCs was used to determine the average relative amount of exchanged thiolate.

2.2 - Preparation of MPC – Doped Xerogel Film Sensors

Preparation of the biosensors was performed using a method established in a previous work[8] to create the sensing scheme depicted in Fig. 1. MPC incorporation into the xerogel has been confirmed with TEM, including cross-sectional TEM, and electrochemistry.[8] UV-Vis analysis of MPC-doped xerogels confirms the MPCs are physically incorporated into the silane network, as they are unable to be completely removed by soaking in pure toluene. After complete drying, 10 μ L of a polyurethane blend of 50:50 (TPU (50 mg):50 HPU (50 mg) in THF) was cast as an outermost semi-permeable membrane and dried for 30 minutes (**Scheme I**).

2.3 - Biosensor Performance and Electrochemical Film Characterization

Prior to testing, sensor constructs were soaked in 4.4 mM potassium phosphate buffer solution (pH = 7.0) for at least one hour. All biosensors were subjected to +0.65 V in 25 mL of PBS for 20 minutes to stabilize the sensor reading. During testing, 25 μ L aliquots of 1 M glucose stock solution were injected at 100 second intervals while stirring to obtain steady state response to successive 1 mM glucose increases. As in prior work, slopes of calibration curves (i.e., current response vs. glucose concentration) corresponded to sensitivity while response times ($t_{R-95\%}$) were defined as the time it takes to reach 95% of the total change in current due to an increase in glucose concentration.[5, 8][5, 8] Permeability indices (PI) were generated in prior studies in this lab[8] and others[22] where the amperometric response of a species at a modified electrode was in ratio

with its response at a bare electrode. Electrode surface areas (potassium ferricyanide) and diffusion coefficients (H_2O_2 and glucose) were measured via chronocoulometry as previously described[23, 24] using the slope of Anson plots and the following equation:

$$Q = 2nFACD^{1/2}\pi^{-1/2}t^{1/2} \quad (1)$$

where Q is the charge passed (C), n is the number of electrons transferred, F is Faraday's constant (96,500 C/mole), A is the electroactive area (cm^2), C is the concentration (mol/cm^3), D is the diffusion coefficient (cm^2/sec), and t is the time (sec).

As with other 1st generation amperometric biosensors,[25] the dynamic range of current responses for MPC-doped xerogel configurations largely followed Michaelis-Menton kinetics with parameters determined from non-linear regression analysis of the following equation:

$$I_s = \frac{I_{\max}}{1+K_m/[S]} \quad (2)$$

where I_s represents amperometric current signal, $[S]$ is substrate concentration (e.g., glucose concentration), I_{\max} is the current plateau or maximum current response obtained when all the film's active enzyme sites are saturated, and K_m is the apparent Michaelis constant signifying the substrate concentration that yields half the maximum amperometric response. K_m values will be sensitive to enzyme access/binding whereas I_{\max} variations under constant experimental conditions reflect differences in the available active enzyme.[25]

2.4 - Electronic Conductivity Measurements

Solid-state conductivity measurements were performed using gold micro-printed interdigitated array (IDAs, MSA Company) electrodes (50 Au fingers, 15 μm finger width, 15 μm gap (d_{gap}) between fingers, 4800 μm finger length, 0.1 μm finger height) – see Supporting

Information (Fig. SI-4). IDAs were treated as parallel plate electrodes, with the total areas of electrode fingers facing one another across defined gaps as represented by $A_{\text{total}} = A_{\text{finger}} (N-1) = 4.8 \times 10^{-6} \text{ cm}^2$, where $N = 50$, and $A_{\text{finger}} = (\text{length}) \cdot (\text{height})$. IDA geometric cell constant (gap distance/ A_{total}) is 6.3 cm^{-1} . [26, 27] Teflon-coated wire was attached to the IDA surface using an Ag epoxy (Stan Rubinstein Associates, Inc.; 65°C ; $> 3 \text{ hrs.}$) and insulated with Epoxy Patch 1C (Henkel North America; 65°C ; $> 3 \text{ hrs.}$). Resistive current measurements generating current-voltage (I-V) curves between $\pm 1.0 \text{ V}$ were conducted with the WE as one IDA lead and the CE and RE connected to the other IDA lead. As received and MPC-coated IDAs were cleaned with acetone/toluene soaking ($> 15 \text{ minutes}$), brief exposure to boiling toluene, and rinsing (EtOH and acetone) whereas xerogel-modified IDAs were discarded after single measurements. Film electronic conductivity (σ_{EL}) was obtained from the slope ($\Delta I/\Delta V$) of the linear portion of the I-V curves ($\pm 200 \text{ mV}$) and calculated using the following relationship: [26, 27]

$$\sigma_{\text{EL}} = d_{\text{gap}}/A_{\text{total}} \cdot \Delta I/\Delta V \quad (3)$$

where $d_{\text{gap}}/A_{\text{total}}$ is the geometric cell constant and $\Delta I/\Delta V$ is the slope of the I-V curve.

3. RESULTS AND DISCUSSION

The successful MPC doping of xerogel scaffolds within 1st generation biosensing schemes was established in prior research (**Scheme I, Figure 1**) and represents the starting point for our current study focused how MPC properties contribute to sensing performance of the scheme. MPC infused xerogel biosensors were extensively characterized, tested for glucose detection, and compared with other sensing schemes in the literature. [8, 17] Specifically, MPC infusion into

xerogels created a dramatic, order of magnitude increase in sensitivity, measured as the slope glucose response calibration curves. Additionally, MPC doping resulted in response times ($t_{R-95\%}$), the time it takes for a glucose response to reach 95% of its total signal, a factor of 4 lower while doubling the linear range of the calibration curve. As illustrated in Fig. 1, calibration curves show solid or bolded markers representing the linear range of the step-response toward increasing glucose concentration whereas the open symbols represent the dynamic range - response that, while still increasing with glucose concentration is no longer yielding clear step-wise responses unique to a specific glucose concentration. During that study,[8] a sensing mechanism was hypothesized to explain the observed enhancements: glucose permeates the outer PU layer, diffuses into the porous xerogel structure where it reacts with embedded GOx and is converted to H_2O_2 , a enzymatic reaction by-product subsequently oxidized at a nearby MPC cores and communicate to the working electrode via fast electron hopping (**Scheme I**). The following study attempts to follow-up that work with an MPC focused investigation of critical structure-function relationships that either promote or diminish the enhancement observed with MPC-doping and further elucidate this proposed sensing mechanism.

The MPC properties of interest and thus the major sections of the paper herein include peripheral ligand chain length and functionality, as well as the NP core size. Systematic manipulation of these MPC properties should allow for identification of the most important MPC characteristics for their incorporation into xerogels and sensing of glucose. It follows then that the three highlighted sensing performance parameters (sensitivity, response time, linear range), traditionally reported for biosensors,[8] can serve as a useful diagnostic for establishing the most important MPC properties if they are encapsulated within xerogels for sensing purposes. The MPC properties that provide the highest sensitivity and linear range at relevant concentrations are of

most interest for glucose biosensing but a greater fundamental understanding of critical MPC structure-function relationships allows for corroboration of the proposed sensing mechanism while also promoting adaptation of the materials/strategy toward sensors for other physiological targets of clinical relevance, the ultimate goal of our work.

3.1 - Chain length of the MPC Peripheral Ligands

MPCs with peripheral skins composed of methyl-terminated (unsubstituted) alkanthiolate ligands varying in chain length, including butanethiolate (C4), hexanethiolate (C6), octanethiolate (C8), decanethiolate (C10), and dodecanethiolate (C12), were doped into MPTMS xerogel films with GOx and tested for their response toward glucose. As illustrated in **Figure 2**, two significant effects were observed with these experiments (**Table 1**, 1st section). First, as the chain length of the peripheral ligands around the gold cores was increased, a significant decrease in the performance sensitivity of the sensor was observed (Fig. 2A). Secondly, a notably sharp increase in response time ($t_{R-95\%}$) was recorded at longer chain lengths (Fig. 2B). Analysis of the calibration curves for the systems with varying peripheral ligand chain lengths reveals that the highest sensitivity (i.e., the system with the greatest current response toward glucose) is the C4 MPCs, the shortest chain length (Supporting Information, Fig. SI-5). K_m and I_{max} determinations for the dynamic range of these systems (Table 1, 1st section) reflect a similar trend where the C4 and C6 doped films exhibit relatively low K_m values while maintaining substantial maximum current. While other chain lengths displayed smaller K_m (e.g., C12 MPC doping) or higher I_{max} (e.g., C8), they were coupled with extremely low current or high values of K_m , respectively.

These results collectively suggest one of a few possibilities regarding the enzymatic reaction believed to be taking place within the film (Scheme I). By increasing the thickness of

the peripheral layer surrounding the cores of the MPCs, it may be hindering the diffusional approach of (a) glucose to the embedded enzyme or (b) H₂O₂ to the NP network where it is oxidized and reported to the electrode. A third possibility is that the larger MPC chain length may be increasing the effective inter-particle distance within the MPC network, an effect observed in other MPC studies.[26-28] Less effective interdigitation of the alkanethiolate ligands from neighboring MPCs necessitates greater particle-to-particle distances within the network that may then disrupt electron hopping connections to the working electrode and decrease peroxide oxidation reporting throughout the film.

In order to assess the diffusion of glucose, which is hydrodynamically delivered to the film interface and diffused within the film, and H₂O₂, which is both generated and diffuses within the xerogel layer, the role of the outer PU layer must first be considered. In terms of H₂O₂ permeability, as previously shown[8], the 50:50 blend of PU employed in these schemes has poor H₂O₂ permeability (<2%, Supporting Information, Fig. SI-6) and may serve to confine the H₂O₂ within the film and limit diffusional loss before oxidation. Regardless of the xerogel system being tested, however, H₂O₂ permeability from external injection is always significantly decreased by the PU layer (Supporting Information, Fig. SI-6). Conversely, values for the diffusion coefficient of glucose (D_{gluc}) for various systems with and without the PU layer, do not show the same drastic difference (Supporting Information, Fig. SI-7). These results suggest that the PU is not as substantial a diffusional barrier for glucose as it is for H₂O₂. With an understanding of the outer PU layer, the MPC-doped xerogel layer can be systematically examined.

Chronocoulometry measured values for the diffusion coefficient of H₂O₂ (D_{H₂O₂}) and D_{gluc} in phosphate buffer at a bare platinum electrodes were 2.3 x 10⁻⁶ cm²/s and 4.8 x 10⁻⁶ cm²/s, respectively, and are in excellent agreement with the literature (D_{H₂O₂} = 1.3 x 10⁻⁵ cm²/s); D_{gluc} =

$5-7 \times 10^{-6} \text{ cm}^2/\text{s}$)[29]. The values drop considerably when they are measured for MPTMS xerogel matrices with or without C6 MPC doping (Table 1), analogous to what is observed for glucose through a Nafion membranes ($D_{\text{gluc}} = 3.4 \times 10^{-8} \text{ cm}^2/\text{s}$) that have been employed for glucose sensing schemes[30]. Thus, we expect small D_{gluc} within any xerogel matrix, regardless of the type of MPC being doped. As we compare these parameters for representative MPC-doped xerogels that differ in the chain length of the ligands, C6 MPC vs. C12 MPC doping, we first note significant drops, by one or two orders of magnitude, in both H_2O_2 permeability and $D_{\text{H}_2\text{O}_2}$ (Table 1). Simultaneously, the use of MPCs with longer chain lengths, in this case dodecane thiolate protected MPCs, resulted in significantly smaller measured values of D_{gluc} through the xerogel. Based only on these chain length study results, a defining aspect of the proposed mechanism (i.e., glucose diffusion, H_2O_2 diffusion, or interparticle spacing) that accounts for the signal enhancement cannot be isolated and none can be discounted.

3.2 - Functionalization of the MPC Peripheral Ligands

If one assumes that the MPC peripheral ligands influence the diffusion of glucose and/or H_2O_2 , both small polar molecules, through the film then the systematic functionalization of MPCs with ω -substituted alkanethiols featuring polar end groups should have a significant effect on the performance of the sensor. As shown in the literature,[21, 27, 31] MPCs can be readily functionalized to different degrees via place-exchange reactions (**Figure 3A**). To determine which ω -substituted alkanethiols would likely elicit the greatest effect when exchanged into the MPCs, self-assembled monolayer (SAM) films composed of various functionalized alkanethiolates, including hydroxy, carboxylate, and aromatic substitutions, were electrochemically probed by recording the cyclic voltammetry of potassium ferricyanide (FeCN) and monitoring the

amperometric response to H_2O_2 injections to assess film hydrophobicity and H_2O_2 permeability, respectively. The results of each type of experiment suggested a specific ω -substituted alkanethiol to be incorporated into the MPC periphery. First, in the case of FeCN electrochemistry, one can consider the polar redox probe's interaction with various functionalized SAMs an approximate mimic to the portion of the proposed sensing mechanism where glucose, a polar but electroinactive species, might interact with MPCs peripheral ligands as it diffuses through the xerogel layer embedded with GOx. The results of this experiment (Supporting Information, Fig. SI-7), shows FeCN voltammetry at 6-mercaptohexanol (MHOL) SAMs was nearly diffusional, only slightly different than at a bare electrode. The 6-mercaptohexane (C6) SAM, on the other hand, was significantly blocking toward the hydrophilic probe. Results from this simple SAM model system suggest that, since MHOL SAMs showed the least barrier to promoting the electrochemistry of ferricyanide in solution, the inclusion of MHOL place-exchanged MPCs within the xerogel might result in even greater enhancement of glucose sensing compared to the original C6 MPC doped system. If such an enhancement was observed, it would substantiate that glucose diffusion (Fig. 1B), mimicked here by FeCN diffusion, here, and was critical to the observed performance of the sensor.

In the second set of experiments, amperometric current-time (I-t) scans with injections of H_2O_2 at the same set of SAM-modified electrodes held at +0.65 V showed that films of 6-mercaptobenzoic acid (MBA) exhibited the highest permeability index (31%) while MHOL SAMs yielded one of the smallest permeability index (8.2%) (see Supporting Information, Fig. SI-8).[8, 22, 25] These results suggest that while the MHOL SAMs may be beneficial for polar molecule diffusion through the MPC-doped xerogel (FeCN results), it is not an interface conducive for facile oxidation of H_2O_2 , another critical component of the proposed mechanism (Fig. 1B). Based on

these results, the incorporation of MHOL and MBA-exchanged MPCs into the xerogel sensing system was examined to reveal the relative importance of glucose and H₂O₂ diffusion, respectively, at the embedded MPC-solution interface within the xerogel. Based on the preliminary results from the FeCN voltammetry and H₂O₂ amperometry experiments at the various types of SAMs, MPCs place-exchanged with either MHOL or MBA to varying degrees were incorporated into xerogels, tested for glucose responsiveness, and calibration curves were generated.

In order to evaluate xerogel systems doped with MHOL place-exchanged MPCs, a representative film was tested for H₂O₂ permeability and the apparent diffusion coefficients of both H₂O₂ and glucose through the film were measured (Table 1, 2nd section and Supporting Information, Fig. SI-6,7). Compared to systems with unfunctionalized C6 MPC doping ($D_{\text{H}_2\text{O}_2} = 8.5 \times 10^{-6}$), the $D_{\text{H}_2\text{O}_2}$ decreased an order of magnitude (1.7×10^{-7} cm²/s) while the D_{gluc} remained approximately the same within the MHOL-functionalized MPC doped xerogel films. These results suggest that if improved sensor response can be achieved by doping the films with MHOL functionalized MPCs, the diffusion of glucose, which is greatly improved within such films, is critical for the sensing mechanism. Fig. 3B shows the calibration curves of various xerogel films doped with MPCs place-exchanged with MHOL at 0%, 18%, 26% and also compared to films with no MPCs (control) as well as with 100% MHOL MPCs synthesized as previously described.[31] Calibration curves in this study are presented with the current response over glucose concentrations from 0 to 28 mM even though the physiologically relevant concentration is from 4-7 mM.[1] When compared to the original C6 MPC films, it appears that any substitution of MHOL ligands into the periphery of the MPCs results in a decrease in sensor performance, most notably in linear range, response time, step response, and, to a lesser extent, sensitivity (**Table 1**, 2nd section). These results suggest that the functionalization of the MPC-doped xerogel with polar

MHOL groups on the ligands does not result in improved diffusion of the polar, hydroxyl functionalized glucose molecules, even though FeCN voltammetry and D_{gluc} measurements would seem to indicate otherwise. While prior research has shown that MHOL functionalization often provides a more hydrophilic environment[17, 31] that one may think is more favorable interaction/diffusion with polar, hydroxyl-functionalized glucose, it did not lead to further enhanced sensitivities etc..

A similar approach was applied with doping the films with MBA-exchanged MPCs, the second type of ligand suggested by the SAM experiments because it exhibited the highest H_2O_2 permeability (Supporting Information, Fig. SI-9). In this case, however, a representative xerogel embedded with MBA-exchanged MPCs showed a substantial increase in H_2O_2 permeability from ~3% to ~20%, mirroring the SAM permeability SAM, as well as a significant increase in D_{gluc} compared to C6 MPC doped xerogels (from 2.15×10^{-7} to 3.3×10^{-6} , see Table 1, 2nd section). Unfortunately, however, a result similar to that of the MHOL exchanged materials was observed for any degree of embedding MBA-exchanged MPCs which all resulted in decreased performance (Supporting Information, Fig. SI-10). Indeed, poor sensing performance was observed for not only embedding MBA functionalized MPCs into the xerogel but also for the use of a significant number of other place-exchanged MPCs as well, including ligand exchange of MPTMS (Supporting Information, Fig. SI-11) and thioctic acid (TA) (not shown). In each case, the use of place-exchanged, functionalized MPCs resulted in diminished sensing performance in at least one major sensing attribute (i.e., lower sensitivity (calibration curve slopes), smaller linear ranges and more limited step-responses) while also exhibiting greater variability compared to the performance of un-substituted C6 MPC-doped films. Michaelis-Menton analysis of the dynamic range of these place-exchanged MPC systems (Table 1, 2nd section) shows that any substitution of ligands for

functionalized ligands (i.e., MBA or MHOL) has an adverse effect, increasing K_m and/or decreasing I_{max} . Here again, the C6 MPC-doped system remaining the most optimal of these systems.

Based only on evaluating sensor performance, K_m/I_{max} modeling, and measurement of permeability, $D_{H_2O_2}$ and D_{gluc} , all the MPC functionalization results suggest that glucose diffusion and/or H_2O_2 permeability at the MPC interface may not be as critical to the sensing mechanism as other factors, particularly the aforementioned interparticle spacing within the film. To explore the effect of chain length/functionalization on edge-to-edge interparticle distance (δ), the solid-state electronic conductivity (σ_{EL}) of various MPC films was examined using interdigitated array (IDA) electrodes as previously described (see Supporting Information SI-5 for more detail).[26, 27, 32] MPC films were drop-cast from toluene solutions onto IDAs and a current-voltage (I-V) curves were collected and used to determine factors controlling film conductivity. In the first case, MPC films of increasing alkanethiolate chain length were drop-cast onto IDAs and measured. We note that, overall, the drop-cast MPC films exhibited significantly lower σ_{EL} compared to similar measurements on larger MPC (Au_{309}) drop-cast films with variable chain length protection,[26] mixed-valent MPC films (Au_{140}),[26] and metal-linked MPC film assemblies (Au_{140}).[27, 32] In the current study, as expected,[26] the MPC (Au_{225}) films comprised of C4, C6, C8, and C10 alkanethiolate protection showed an significant decrease in σ_{EL} with increasing chain length (**Figure 4**). The exponential decay in σ_{EL} (Fig. 4B) is consistent with an electron tunneling mechanism through trans-staggered alkane chains in accordance with the following relationship:

$$\sigma_{EL} = \sigma_{n=0} \exp [-n\beta_n] \exp [-E_a/RT] \quad (4)$$

where n is the alkanethiolate chain length, $\sigma_{n=0}$ is the extrapolated conductivity at zero distance ($n=0$), E_a is the activation energy at the temperature (T), R is the gas constant, and β_n is the mechanistically instructive electronic coupling term (beta decay).[26] With the conductivity of these films differing in chain length, two cases are simultaneously considered: (1) MPCs separated by a minimum distance where $\delta = n$, the length of the alkanethiolate ligand in number of carbons (i.e., complete interdigitation of neighboring MPC ligands); and (2) MPCs are separated by a maximum distance where $\delta = 2n$ (i.e., no interdigitation) (Fig. 4B, inset). In these cases, the results show β_n of 1.7 and 0.87 per methylene carbon unit (CH_2^{-1}), respectively. Based on prior studies of films of slightly larger or smaller MPCs by Murray et al.,[26, 27, 32] these values convert ($1.5 \text{ \AA}/\text{CH}_2$) to more traditional distance-based β_{dis} of 1.2 \AA^{-1} and 0.6 \AA^{-1} . With the actual interdigitation between these extremes but known to be *nearly* fully interdigitated from prior work,[26, 27] these results are in agreement with an electron tunneling mechanism, similar to electron transfer (ET) of redox proteins[33] or ferrocene[34] at well-ordered SAM modified electrodes ($0.8\text{-}1.2 \text{ \AA}^{-1}$). Given the exponential decay of electrons over distance, it suggests that MPC networks will be extremely sensitive to the edge-to-edge separation of MPCs.

Solid-state conductivity measurements were also used to study the effect of MPC functionalization within these systems. Films of MHOL place-exchanged MPCs (drop-cast from ethanol solution) exhibited a systematic decrease of conductivity with increasing MPC MHOL content (Fig. 4A and 4C) though not as drastic as the chain length effect. It is suggested that the exchange of ω -substituted alkanethiols into the MPC periphery results in less effective interparticle ligand interdigitation since the polar end groups of one MPC would have to insert among the hydrophobic alkane back-bones of an adjacent MPC. As a result of this forced interaction, it is expected that the interparticle distance (δ , Fig. 4C, inset scheme) will necessarily be larger and

decrease σ_{EL} . Conductivity results for MPC ligand chain length and functionality are summarized in the first two sections of **Table 2**. It has been established that ET through assembled films of MPCs can occur via an “electron hopping” mechanism and can occur over significant distances without decay.[8, 31, 33] The films studied here are solid-state MPC films and may not be analogous to MPC-doped xerogels. If, however, the ET mechanism through the MPC networks of the xerogel films is occurring via a hopping mechanism as suggested, it follows that increasing interparticle distance with thicker or functionalized peripheral ligands would necessarily disrupt electronic coupling between particles and result in degraded performance even if such peripheral functionality provides hydrophobic/hydrophilic properties conducive to the targeted analyte (glucose) and/or enzymatic reaction product (H_2O_2).

While the incorporation of most ligand exchanged-MPCs resulted in decreased sensing performance and lower conductivity, an interesting result occurred when 6-mercaptophenol (MPOL), a ligand combining the hydroxyl functionality of MHOL with the aromaticity of MBA, was used. In this case, FeCN voltammetry and H_2O_2 permeability at the MPOL SAMs showed highly diffusional voltammetry and significant amperometric response, respectively (Supporting Materials, Fig. SI-11). During σ_{EL} measurements, the MPOL-functionalized MPCs were also the only material tested to yield a trend of increasing σ_{EL} with increasing ligand exchange, opposite of MHOL and MBA substituted materials (Table 2 and Supporting Materials, Fig. SI-11). While the MPOL-exchanged MPC-doped xerogels still exhibited lower sensitivity than unfunctionalized MPC-doped films, the films also showed a unique and significant improvement in step response definition and an elongated dynamic range compared to any other place-exchanged MPCs in xerogels (Supporting Materials, Fig. SI-11). The improved step-response to greater glucose concentrations is not yet well understood but may very well be due to improved H_2O_2 permeability

and diffusion within the MPOL-exchanged MPC doped films, though the dominant factor in the overall sensing mechanism still appears to be the interparticle spacing.

3.3 - MPC Core Size

One approach to probing the ET through these films, the diffusion *independent* aspect of the proposed sensing mechanism, is to systematically alter the core size of the MPCs being incorporated into the xerogel films. Electrochemical properties of MPC-type nanoparticles are categorized into three different regimes: (1) bulk metal continuum behavior for larger particles (>3-4 nm diameter); (2) metal-like capacitor behavior with observable quantized double layer (QDL) charging for smaller particles (~1.5-3 nm in diameter) and; (3) very small particles (<1.5 nm in diameter) with molecule-like behavior, namely significant HOMO-LUMO and electrochemical energy gaps.[35] ET through films of the intermediate MPC regime (e.g., Au₁₄₀C₆₇₀) have been extensively studied to establish exceptionally high rates of electron hopping (e.g., $2 \times 10^6 \text{ s}^{-1}$) and electron self-exchange rates (e.g., $2 \times 10^8 \text{ M}^{-1}\text{s}^{-1}$).[36] Our own study of ET of redox proteins at dithiol-linked MPC film assemblies showed undiminished protein ET rate constants even over significant film thicknesses.[8, 31, 33] In the present study, C6 MPCs with diameters that span the first two size categories of MPCs were synthesized according to existing procedures[20] and doped into the xerogel films with embedded GOx (Fig. 1). The motivation of this core size study was to see if sensing film performance is affected by MPC core size thereby identifying the optimum core size that provides enhanced sensing response as well as the properties of MPCs that perpetuate the sensing mechanism.

Figure 5 represents typical current-time (I-t) amperometry for glucose injections at xerogel films embedded with GOx and doped with MPCs of varying sizes including MPCs with the

following *average* estimated core sizes: Au₇₉, Au₁₄₀, Au₂₂₅, Au₃₁₄, and Au₄₇₉₄ – materials with average core diameters ranging from ~1.2, at the edge of the molecular-behavior regime, to ~5.0 nm, well within the bulk metal behavior regime (see Supporting Information, Fig. SI-12-15).[35] The results illustrate a dramatic degradation in performance of films with the largest cores, Au₄₇₉₄ including poorly resolved and limited step response, lower sensitivity, smaller current and increased response time. MPCs of the second core size category (Au₇₉, Au₁₄₀, Au₂₂₅, and, to a lesser extent, Au₃₁₄) all exhibited enhanced sensing responses (i.e., well-defined step responses, large linear/dynamic ranges, and improved response times) compared to the larger cores or films without MPCs. As established in prior work,[8] sensor performance with xerogels that are not embedded with MPCs was poor, exhibiting limited step responses as well as longer response times and a limited linear range. The performance properties of these sensor systems are summarized in Table 1 with corresponding calibration curves included in Supporting Information, Fig. SI-17.

Solid-state σ_{EL} measurements on drop-cast MPC films of varying core sizes (Table 2, 3rd section) are consistent with the aforementioned sensor results. As shown in Fig. 5B, the intermediate core MPCs (Au₇₉, Au₁₄₀, Au₂₂₅ and Au₃₁₄) all show similar and expected σ_{EL} [26, 27][32], significantly different from that of the larger core film (Au₄₇₉₄). Of the intermediate cores, it is not yet firmly understood why the Au₂₂₅ are consistently the most conductive and optimal in performance.

Taken in conjunction with each other, the amperometric responses of MPC-doped xerogels and the σ_{EL} of MPC drop-cast films as a function of core size, suggest that the sensing response is indeed dependent on core size. The inference is that the use of MPCs known to exhibit quantized charging effects,[35] metal-like MPCs, is necessary to achieve the enhanced sensing attributes. It follows that the electron hopping known to occur through MPC films with cores in that size regime

must be an important component of the sensing mechanism, one that is critically reliant on the particle-to-particle electronic coupling in order to report electrochemical reactions occurring throughout the film.

3.4 - Composite Xerogel-MPC Films

This report has, to this point, focused on specific individual components within the biosensing scheme, including the MPC core and ligand periphery. In this last section, the composite MPC-xerogel film is examined in more depth. So far, the results presented suggest that the most important factor in the sensing mechanism of highly performing MPC-doped systems is the electronic communication within the MPC network that reports oxidation of H₂O₂ throughout the film. The MPC enhanced performance often includes greater linearity, higher sensitivity, extended dynamic step responses (step-response), and faster response times. If the enhancement is indeed derived from the presence of an electronically coupled MPC network, it follows that there should exist a critical concentration of MPCs to achieve that effect - a percolation threshold.

If the xerogel films are formed with varying ratios of MPC-to-silane, from no MPC doping (i.e., 100% silane or “no MPCs”), through diluted MPC incorporation (e.g., 1:3200 ratio), and to the doping maximum at the solubility limit of 1:400, the nature of the composite film significantly changes. Cyclic voltammetry of ruthenium hexamine (RuHex), a commonly employed polar redox probe, at xerogel interfaces with no PU layer and varying MPC content suggests the film is either significantly less porous or significantly more hydrophobic. That is, RuHex is increasingly blocked with increasing MPC doping (Supporting Information, Fig. SI-18). It follows that tracking xerogels doped with varying concentrations of MPCs may reveal a percolation threshold for enhanced sensing.

Figure 6A shows a typical result from these varying MPC-to-silane ratio experiments. The figure displays that there is a clear abrupt increase in sensitivity of the sensors between the ratios of 1:6400 and 1:3200 (Fig. 6A). Unfortunately, we have found that while these experiments nearly always reveal a percolation threshold, the exact ratio defining that threshold is somewhat variable experiment-to-experiment, ranging from ratios of 1:3200 down to 1:128,000. Ratios between 1:400 (maximum) and 1:1600 consistently showed enhanced sensing while the lowest ratios of MPCs approached the poor behavior of films without MPCs. MPC-doped xerogels were also measured for σ_{EL} via drop-casting films onto IDA as previously described (Table 2, 4th section). The measurements show that the un-doped xerogel film (i.e., no MPCs) is orders of magnitude less conductive than the 1:400 doped films. Composite films with higher doping levels between 1:600 and 1:800 exhibited similar σ_{EL} while those with low doping levels (e.g., 1:2400 or 1:6400) are more similar to the σ_{EL} of pure xerogel films, again suggesting but not adequately defining a percolation threshold. That stated, even this rudimentary evidence of a percolation threshold within these experiments supports the notion that the electronic coupling of the MPCs within the xerogel is a critical component to the sensing mechanism.

The apparent core-size dependency for the sensing performance of these materials and the suggestion that it is related to MPCs that exhibit QDL charging behavior prompted further study of the composite films. With gold cores surrounded with an alkanethiolate periphery, MPCs with core diameters of 2 nm or less exhibit QDL charging behavior because of their inherently low (sub-attofarad) cluster capacitance (C_{CLU}). The low capacitance allow for single electron transfers (SETs) to occur at large, discrete voltage intervals ($\Delta V = e/C_{CLU}$) that are electrochemically observable at room temperature with cyclic voltammetry and/or differential pulse voltammetry (DPV). This phenomena has been observed in non-aqueous solutions of MPCs[35-39] as well as

with monolayer[38] and multi-layer MPC film assemblies[37] with the only requirement being that the core size is small and reasonably monodisperse.[35]

In **Figure 6B**, a comparison of DPV of systems relevant to this study is presented. A bare Pt electrode immersed in a 0.1M TBAP/CH₂Cl₂ solution yields a relatively featureless response. The same electrode immersed in a solution of C6 MPCs (Au₂₂₅) reveals QDL charging peaks consistent with what is expected from a somewhat polydisperse sample of MPCs, typical of as-prepared samples from an unmodified Brust reaction synthesis.[40] Interestingly, QDL charging peaks are also achieved with MPC-doped xerogels in TBAP/CH₂Cl₂ solution. In comparing the DPV response for the xerogel film with that of the solution MPCs, several notable observations can be made. First, the similarity in magnitude of the two signals suggests that multi-layers of MPCs must be electronically coupled within the xerogel film, consistent with proposed mechanism discussed. Second, z-plot analysis[35, 40] of peak potentials versus MPC charge state confirm that the MPC population producing the observable QDL charging peaks are the same in each case. The average peak spacing (i.e., slope of z-plot) for the MPC-doped xerogel (0.275 V) and the MPC solution (0.267 V) yields C_{CLU} of 0.58 aF and 0.60 aF, respectively. These capacitance values are consistent with MPC core diameters between 1.7-1.9 nm,[40] a characteristic confirmed by our TEM/histogram analysis (Supporting Information). Third, the DPV of the xerogel film is noticeably more defined, lacking the “double peaks” of the solution C6 MPC sample at 0.0, 0.5, and 0.8 V, for example. One can speculate that the porous xerogel may be trapping certain sized MPCs within the network while allowing other, perhaps smaller, MPCs populations to diffuse from the xerogel. Such a scenario would be consistent with the observed decrease in UV-Vis signal upon immersion in an organic solvent (see Supporting Information, Fig. SI-2). It should be noted that the QDL charging peaks shown for the MPC-doped xerogel in Fig. 6B is not a typical

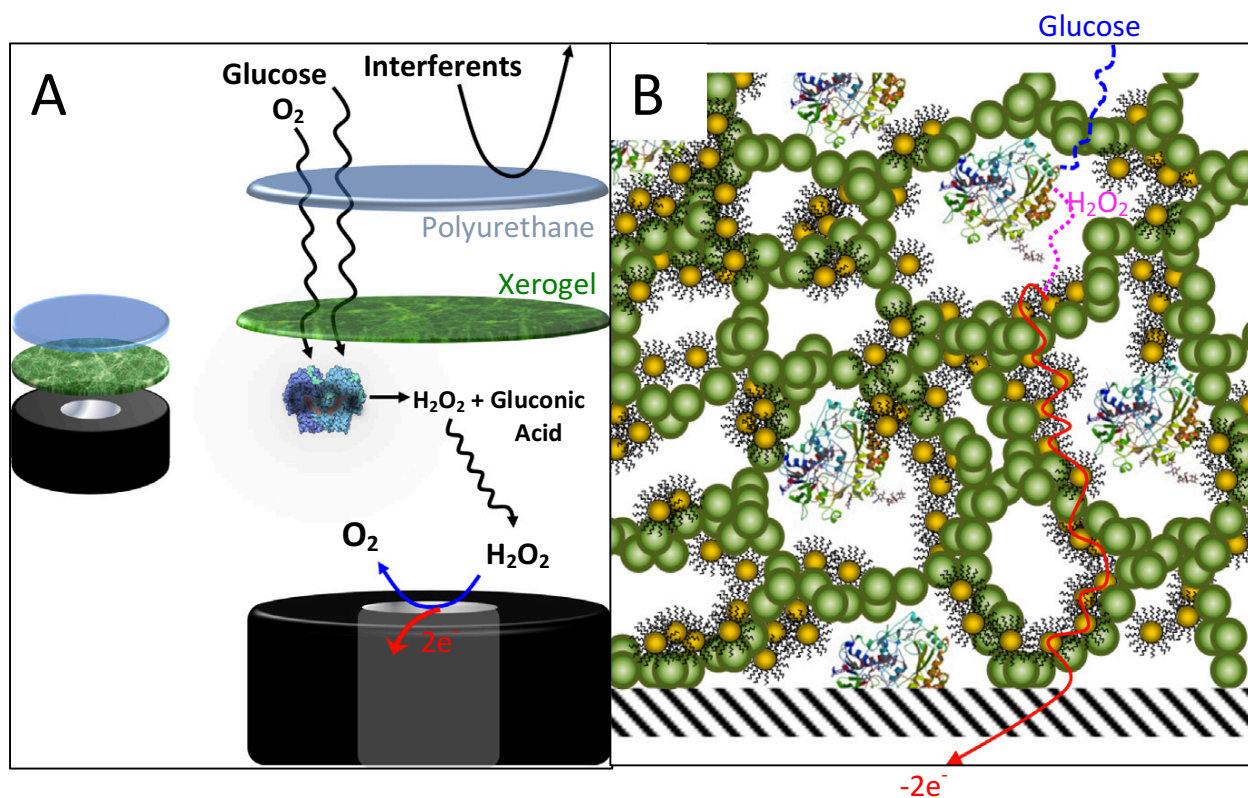
result. Unfortunately, clearly defined QDL charging peaks were more often difficult to achieve repeatedly, challenging to assign specific peaks for z-plot analysis, and prohibited direct calculation of ET rate constants which require an electrochemical signal of ET. While evidence of QDL peaks is readily observed with MPC-doped xerogels, the peak definition presented in Fig. 6B represents of most defined result to date, including a well-formed trough marking the potential of zero charge. Other, more typical, examples of QDL charging peaks for Au₂₂₅ doped xerogel films are included in Supporting Information, Fig. SI-19.

4. CONCLUSION

As the scientific community continues to explore the advantages and disadvantages of incorporating nanomaterials,[3] including metallic NPs,[9, 10] into biosensor strategies, it is important that critical structure-function relationships within the specific schemes are identified so that the strategy may be optimized and a deeper understanding of sensing mechanism be achieved. In this study, those relationships within MPC-doped, xerogel-based, 1st generation amperometric glucose biosensor schemes, systems previously established as producing enhanced sensing performance, were systematically explored in order to define the sensing mechanisms and identify MPC characteristics that may be optimized for sensor development. Specific manipulation of NP core size, peripheral ligand chain length/functionality, as well as, the MPC composition of the overall film, showed that the interparticle spacing of the MPCs within the film and the fast ET that results from an electronically coupled MPC network were the most relevant properties of these MPC-doped xerogels in this regard. The permeability and diffusion of H₂O₂ as well as the diffusion of glucose through the xerogel films, while important, were not found to

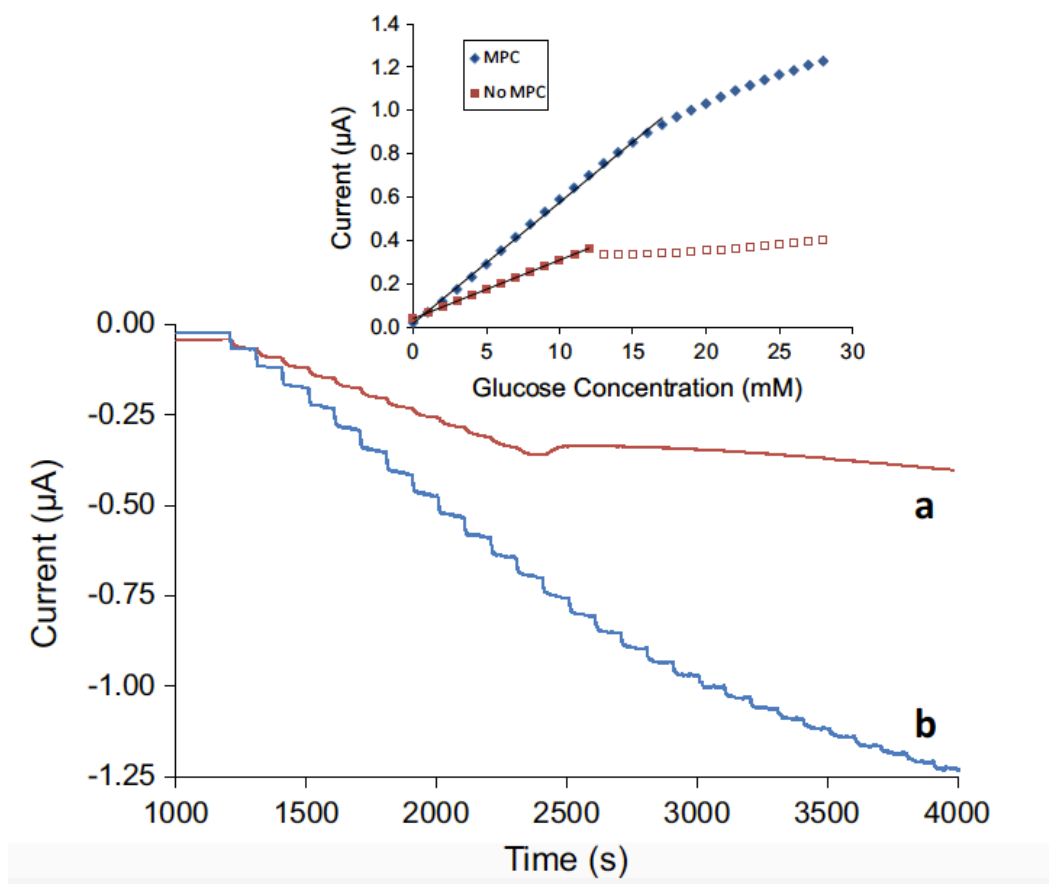
be as critical to the sensing mechanism as the interparticle connections of the MPCs. Infusion of MPCs into the xerogel-based sensing scheme resulted in increased sensitivity, faster response times, and extended linear ranges only when the MPC loading film exceeded a percolation threshold. Any disruption of the interparticle spacing, either via MPC ligand functionalization, increased of the MPC ligand chain length, or dilution of the MPCs within the film, was detrimental. Overall the results support the hypothesized sensing mechanism illustrated in Scheme I - the interconnected MPC network in the xerogel acts as a type of 3-dimensional extension of the electrode surface, allowing the enzymatic reaction generated H_2O_2 to diffuse to any portion of the MPC network, rather than the underlying working electrode for oxidation. The MPC network is able to report the oxidation of H_2O_2 efficiently via fast electron hopping throughout the film, decreasing the scheme's diffusional dependence. This mechanism explains the high degree of enhancement observed compared to the sensors without MPC doping.[8] The findings of this study will be used in future work to apply the general strategy to the additional aforementioned sensing targets that have clinical applications.

APPENDIX



Scheme I. (A) Schematic representation of 1st generation amperometric glucose biosensor scheme with GOx embedded in a MPTMS xerogel capped with polyurethane; (B) Expansion of xerogel component with proposed sensing mechanism where glucose diffuses to MPC-doped xerogel (*blue - dashed*), undergoes an enzymatic reaction with GOx to produce H₂O₂ which subsequently diffuses to the nearest portion of the MPC network (*pink - dotted*) which, in turn, reports H₂O₂ oxidation via fast electron transfer through the MPC network to the working electrode (*red - solid*).

Figure 1.
Examples
of



amperometric $I-t$ curves during successive 1 mM injections of glucose at platinum electrodes modified with **(a)** GOx embedded 3-MPTMS xerogels and **(b)** GOx embedded MPTMS xerogel doped with C6-MPCs, each coated with PU (Scheme I). Inset: Calibration curves for glucose biosensors constructed with platinum electrodes modified with GOx embedded MPTMS xerogels with and without C6-MPC doping where solid markers indicate a step-like response to glucose concentration increases whereas open markers indicate a non-step response (dynamic range). Linear regression has been performed with the linear range shown as a solid black line. Error bars have been omitted for clarity [8].

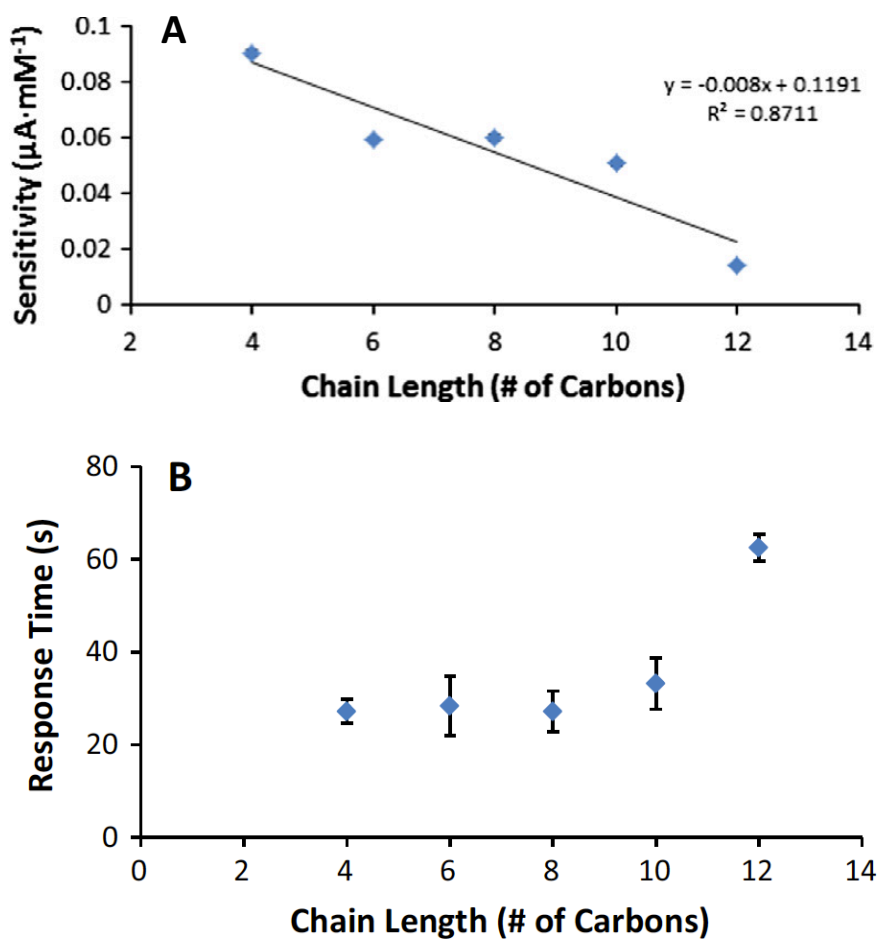


Figure 2. (A) Sensitivity to glucose of the linear range of the calibration curves as a function of the chain length (# of carbons) of methyl-terminated alkanethiolate MPC peripheral ligands within MPTMS xerogel biosensor systems; (B) Response time ($t_{r-95\%}$) of the first 1M glucose injection for each MPC ligand chain length. Note: In some cases, error bars are smaller than markers for average sensitivity.

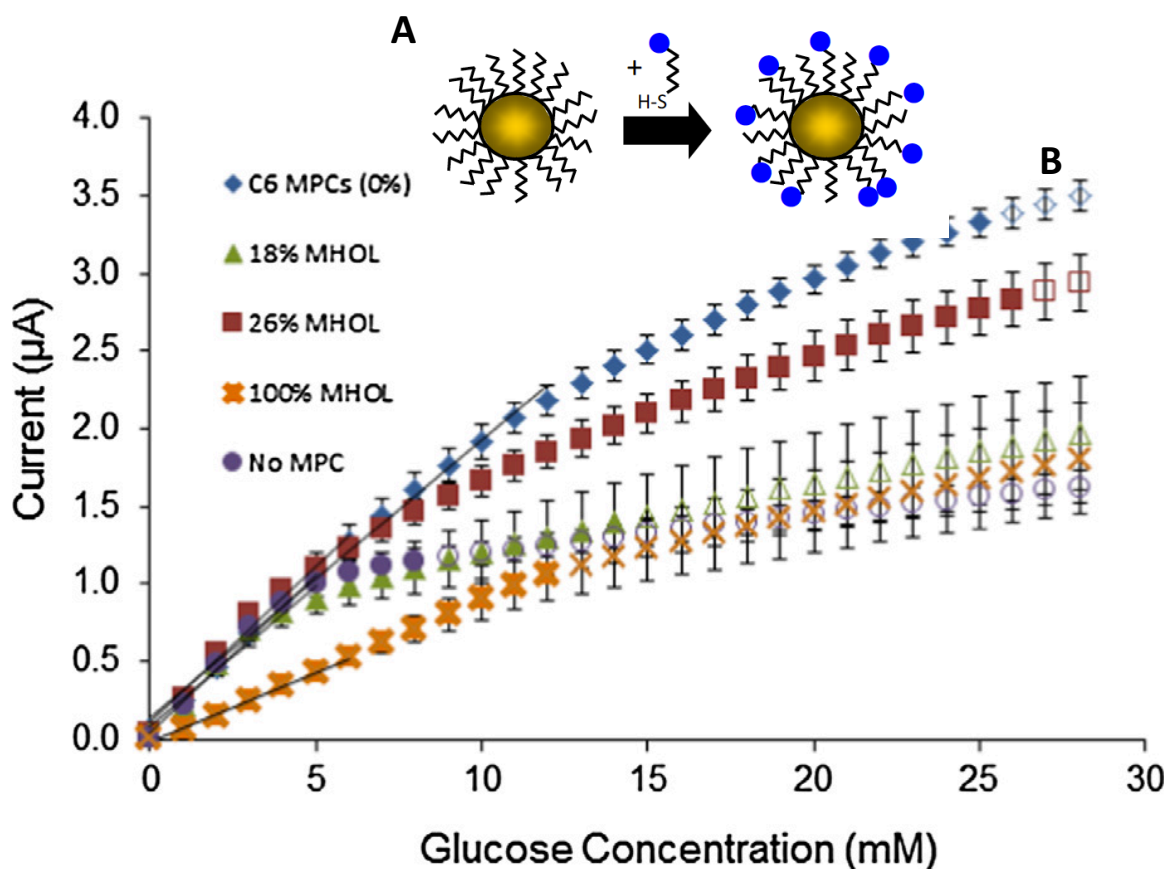


Figure 3. (A) Schematic depiction of place-exchange reactions for functionalizing MPCs. (B) Calibration curves for glucose biosensors constructed at platinum electrodes modified with GOx embedded MPTMS xerogels undoped (●) and doped with C6 MPCs (0%, ◆), C6 MPCs exchanged with MHOL (18%, ▲), C6 MPCs exchanged with MHOL (26%, ■), and MHOL MPCs (100%, X). Solid or bold (X) symbols indicate a step-like response to increases in glucose concentration whereas open symbols indicate a non-step response (dynamic range). All sensors were coated with a PU outer layer. Note: In some cases, standard error bars are smaller than markers for average value.

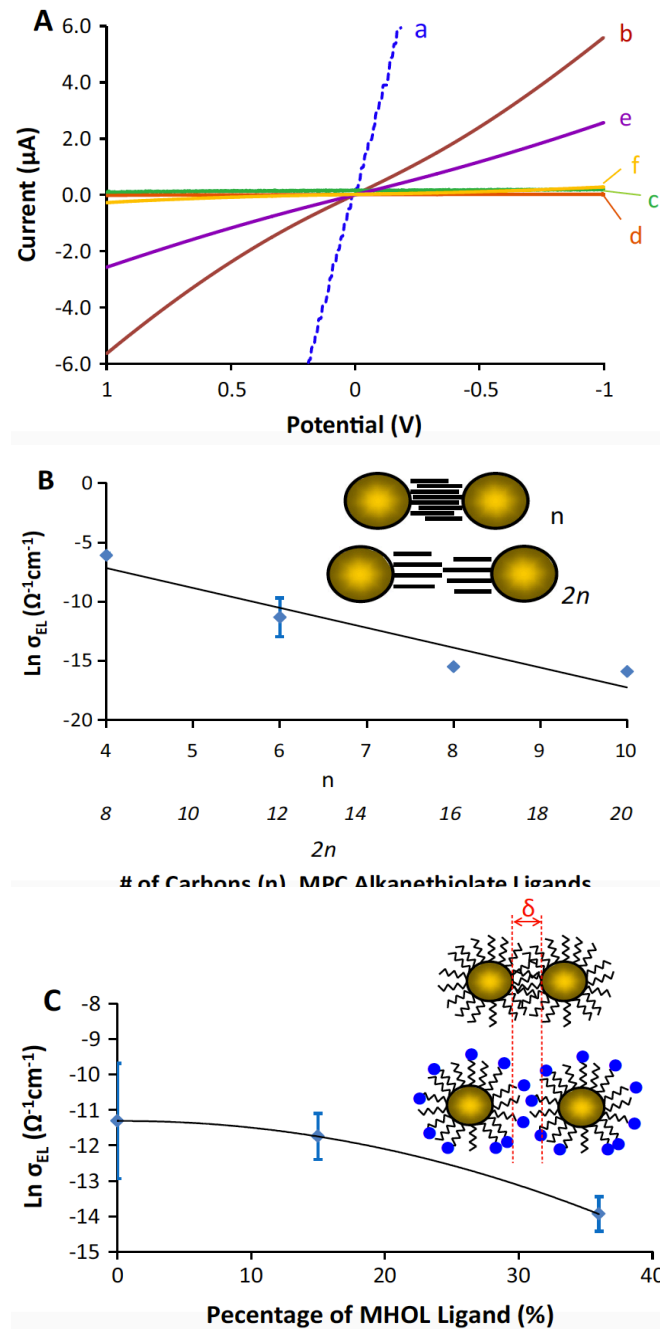


Figure 4. (A) I-V curves for various MPC films on IDA electrodes including films of (a) butanethiolate (C4) protected MPCs, (b) hexanethiolate (C6) protected MPCs, (c) octanethiolate (C8) protected MPCs, and (d) decanethiolate protected (C10) MPCs as well as (e) C6 MPCs with 15% MHOL exchange, (f) C6 MPCs with 36% MHOL exchange. (B) Electronic conductivity (σ_{EL}) of films of C6-protected MPCs deposited on IDA electrodes as a function of the number of carbons in the peripheral protective ligands. (C) Conductivity (σ_{EL}) of films of MHOL-exchanged hexanethiolate-protected MPCs deposited on IDA electrodes as a function of the percentage of ligand exchange with 6-mercaptohexanol (MHOL). Note: In some cases, standard error bars are smaller than markers for average value.

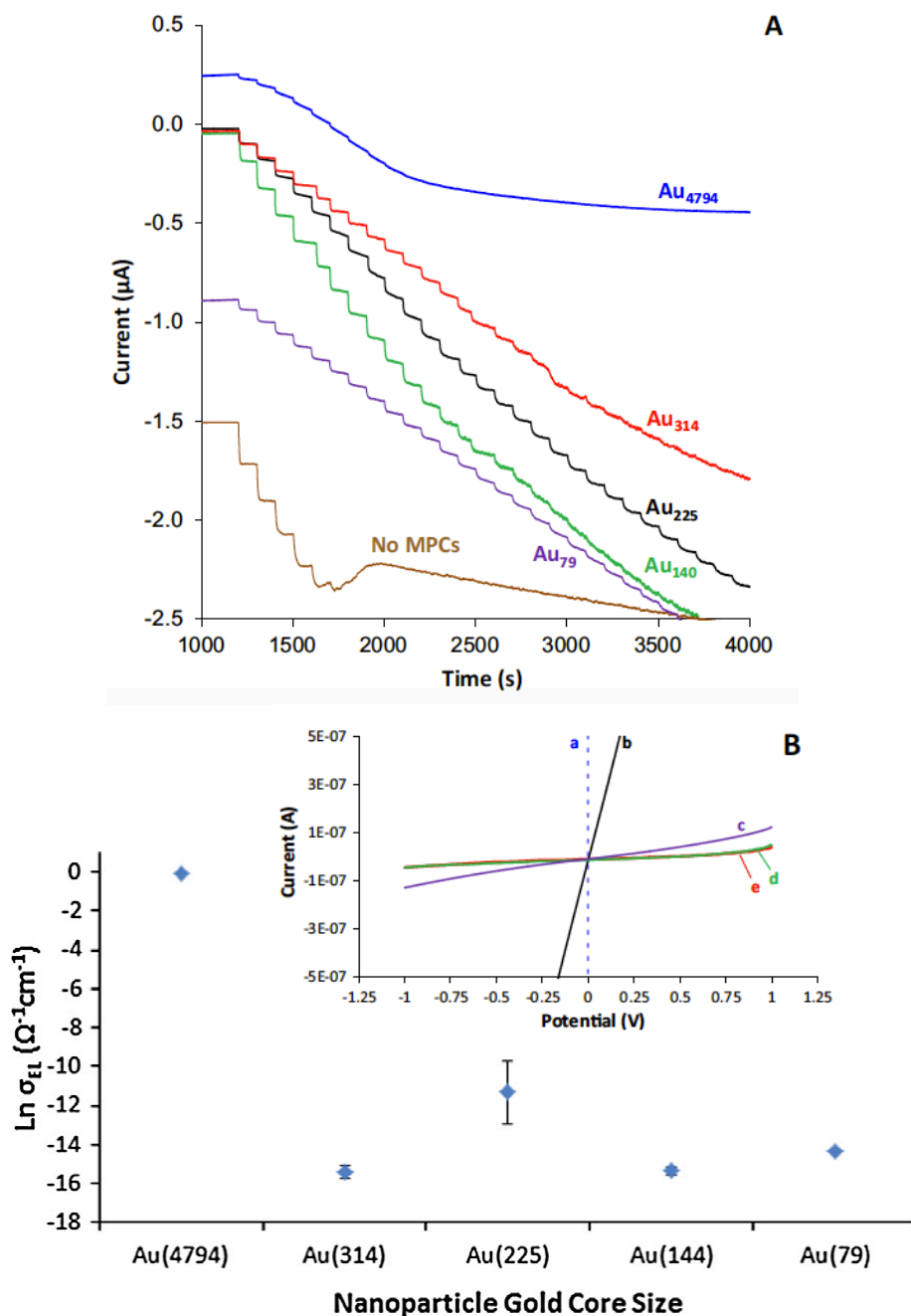


Figure 5. (A) Representative I-t curves during successive glucose injections (1 mM) at electrodes modified with GOx embedded MPTMS xerogel doped with MPCs of different core sizes. Note: Certain I-t curves (No MPCs, Au₇₉, Au₄₇₉₄) are y axis offset from original starting current ($\sim -0.03 \mu\text{A}$) to more effectively illustrate differences in sensing performance/step response. Unmodified results are included in Supporting Information (Fig. SI-14). (B) Electronic conductivity (σ_{EL}) of films of C6-protected MPCs of with corresponding I-V curves (inset) as a function of MPC core size: (a) Au₄₇₉₄, (b) Au₂₂₅, (c) Au₇₉, (d) Au₁₄₁, and (e) Au₃₁₄. Note: In some cases, standard error bars are smaller than markers for average value.

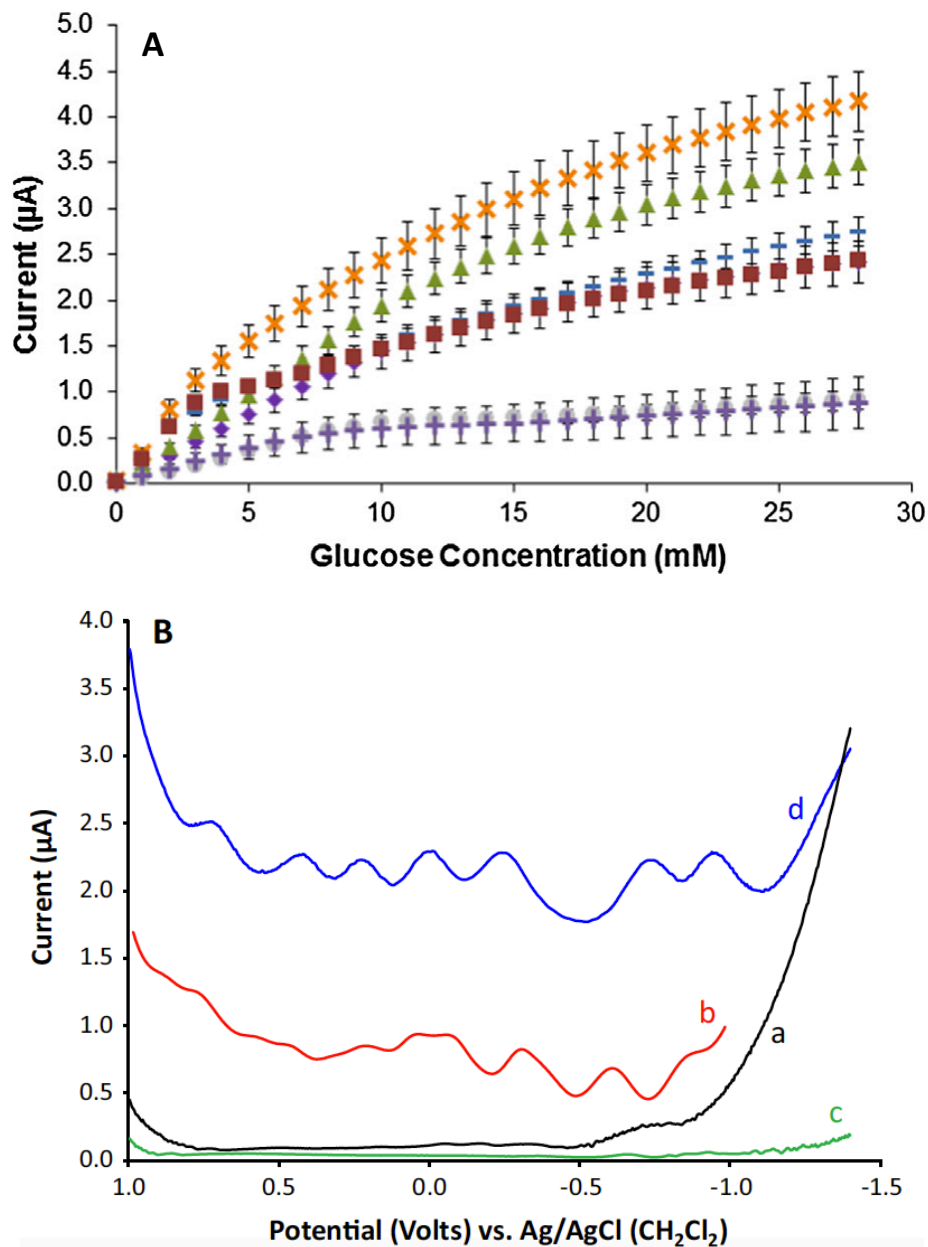


Figure 6. (A) Calibration curves for glucose biosensors constructed at platinum electrodes modified with GOx embedded xerogels with no MPCs (+) and doped with C6 MPCs at a MPC:Silane ratio of 1:400 (◆ and ▲), 1:800 (X), 1:1600 (-), 1:3200 (■), and 1:6400 (●). (B) Differential pulse voltammetry (DPV) of (a) bare Pt electrode, (b) C6 MPC solution, (c) MPTMS xerogel (no MPCs), and (d) MPC-doped MPTMS xerogel (Solution: 0.1 M TBAP/CH₂Cl₂). Note: In some cases, standard error bars are smaller than markers for average value.

REFERENCES

- [1] J. Wang, *Chem Rev.* 108 (2008) 814.
- [2] M. Pohanka, P. Skládal, *Journal of Applied Biomedicine.* 6 (2008) 57.
- [3] K. Kerman, M. Saito, E. Tamiya, S. Yamamura, Y. Takamura, *TrAC, Trends Anal Chem.* 27 (2008) 585.
- [4] U. Narang, P.N. Prasad, F.V. Bright, K. Ramanathan, N.D. Kumar, B.D. Malhotra, M.N. Kamalasanan, S. Chandra, *Anal Chem.* 66 (1994) 3139.
- [5] A. Koh, Y. Lu, M.H. Schoenfish, *Anal Chem.* (2013).
- [6] J.H. Shin, S.M. Marxer, M.H. Schoenfish, *Anal Chem.* 76 (2004) 4543.
- [7] Y. Yang, T. Tseng, J. Yeh, C. Chen, S. Lou, *Sensors Actuators B: Chem.* 131 (2008) 533.
- [8] M.H. Freeman, J.R. Hall, M.C. Leopold, *Anal Chem.* 85 (2013) 4057.
- [9] M. Niemeyer, *Angew Chem Int Ed Engl.* 40 (2001) 4128.
- [10] R. Shenhar, V.M. Rotello, *Acc Chem Res.* 36 (2003) 549.
- [11] G. Sánchez-Obrero, M. Cano, J.L. Ávila, M. Mayén, M.L. Mena, J.M. Pingarrón, R. Rodríguez-Amaro, *J Electroanal Chem.* 634 (2009) 59.
- [12] D. Feng, F. Wang, Z. Chen, *Sensors Actuators B: Chem.* 138 (2009) 539.
- [13] J. Zhang, *Science in China.Series B, Chemistry.* 52 (2009) 815.
- [14] M. Barbadillo, E. Casero, M.D. Petit-Domínguez, L. Vázquez, F. Pariente, E. Lorenzo, *Talanta.* 80 (2009) 797.
- [15] S. Zhang, N. Wang, Y. Niu, C. Sun, *Sensors Actuators B: Chem.* 109 (2005) 367.
- [16] F. Tang, *Science in China.Series B, Chemistry.* 43 (2000) 268.
- [17] N. Poulos, J. Hall, M. Leopold, *Langmuir.* DOI: 10.1021/la504358t (2015) .
- [18] M. Brust, M. Walker, D. Bethell, D.J. Schiffrin, R.J. Whyman, *J Chem Soc - Chem Commun.* (1994) 801.
- [19] T. Doan, M. Freeman, A. Schmidt, N. Nguyen, M. Leopold, *J Visualized Experiments.* 56 (2011).

- [20] M.J. Hostetler, J.E. Wingate, C.-. Zhong, J.E. Harris, R.W. Vachet, M.R. Clark, J.D. Londono, S.J. Green, J.J. Stokes, G.D. Wignall, G.L. Glish, M.D. Porter, N.D. Evans, R.W. Murray, *Langmuir*. 14 (1998) 17.
- [21] R.S. Ingram, M.J. Hostetler, R.W. Murray, *J Am Chem Soc*. 119 (1997) 9175.
- [22] J. Shin, B. Privett, J. Kita, *Analytical Chemistry (AC)*. 80 (2008) 6850.
- [23] A. Bott, W. Heineman, *Current Separations*. 20 (2004) 121.
- [24] D. Campell-Rance, T. Doan, M. Leopold, *J Electroanal Chem*. 665 (2011) 343.
- [25] S.A. Rothwell, S.J. Killoran, R.D. O'Neill, *Sensors*. 10 (2010) .
- [26] W.P. Wuelfing, S.J. Green, J.J. Pietron, D.E. Cliffel, R.W. Murray, *J Am Chem Soc*. 122 (2000) 11465.
- [27] F.P. Zamborini, M.C. Leopold, J.F. Hicks, P.J. Kulesza, M.A. Malik, R.W. Murray, *J Am Chem Soc*. 124 (2002) 8958.
- [28] F.P. Zamborini, L.A. Smart, M.C. Leopold, R.W. Murray, *Anal Chim Acta*. 496 (2003) 3.
- [29] K.G. Stern, *Berichte*. 66 (1933) 547.
- [30] Z. Fan, D.J. Harrison, *Analytical Chemistry*. 64 (1992) 1304.
- [31] A.F. Loftus, K.P. Reighard, S.A. Kapourales, M.C. Leopold, *J Am Chem Soc*. 130 (2008) 1649.
- [32] M.C. Leopold, R.L. Donkers, D. Georganopoulou, M. Fisher, F.P. Zamborini, R.W. Murray, *Faraday Discuss*. 125 (2004) 63.
- [33] M.L. Vargo, C.P. Gulka, J.K. Gerig, C.M. Manieri, J.D. Dattelbaum, C.B. Marks, N.T. Lawrence, M.L. Trawick, M.C. Leopold, *Langmuir*. 26 (2010) 560.
- [34] J.F. Smalley, S.W. Feldberg, C.E.D. Chidsey, M.R. Linford, M.D. Newton, Y. Liu, *J Phys Chem*. 99 (1995) 13141.
- [35] R.W. Murray, *Chem Rev*. 108 (2008) 2688.
- [36] J.F. Hicks, F.P. Zamborini, A.J. Osisek, R.W. Murray, *J Am Chem Soc*. 123 (2001) 7048.
- [37] F.P. Zamborini, J.F. Hicks, R.W. Murray, *J Am Chem Soc*. 122 (2000) 4514.
- [38] J.F. Hicks, F.P. Zamborini, R.W. Murray, *J Phys Chem B*. 106 (2002) 7751.
- [39] J.F. Hicks, D.T. Miles, R.W. Murray, *J Am Chem Soc*. 124 (2002) 13322.
- [40] D.T. Miles, M.C. Leopold, J.F. Hicks, R.W. Murray, *J Electroanal Chem*. 554-555 (2003) 87.

[41] https://www.nigms.nih.gov/Education/pages/factsheet_sepsis.aspx

[42] Ananth, Cande V., and Olga Basso. *Epidemiology (Cambridge, Mass.)* 21.1 (2010): 118–123.

[43] Berry GT. Classic Galactosemia and Clinical Variant Galactosemia. 2000 Feb 4 [Updated 2014 Apr 3]. In: Pagon RA, Adam MP, Ardinger HH, et al., editors. GeneReviews® [Internet]. Seattle (WA): University of Washington, Seattle; 1993-2015. Available from: <http://www.ncbi.nlm.nih.gov/books/NBK1518/>